JOURNAL OF SOLID STATE CHEMISTRY 119, 394–399 (1995)

On the Origin of the Short Interslab Te ··· Te Contacts in the New MA_xTe_2 Phases (M = Nb, Ta; A = Si, Ge; $1/3 \leq x \leq 1/2$)

M. Evain,[1] L. Monconduit, and R. Brec

Laboratoire de Chimie des Solides, I.M.N., UMR CNRS 110, Université de Nantes, 2 rue de la Houssinière, 44072 Nantes Cedex 03, France

Received April 5, 1995; accepted June 8, 1995

The powder pattern characteristics of the new MA_xTe_2 phases (M = Nb, Ta; A = Si, Ge; $1/3 \leq x \leq 1/2$) are analyzed. It is shown that two MA_xTe_2 with very close x values can be easily distinguished solely on the basis of their $0k0$ reflections, which can be singled out in a pattern by intensifying the preferred orientation. The origin of the short interslab Te ··· Te contacts in the MA_xTe_2 compounds is then investigated. The study demonstrates that the short interlayer Te ··· Te contacts (≈3.75 Å) observed in all MA_xTe_2 phases are due to steric effects, regardless of a possible charge transfer. The striking variation of the shortest contacts as a function of x is shown to be directly related to the relative position of the Te atoms within the slabs.

INTRODUCTION

The layered phases MA_xTe_2 (M = Nb; Ta; A = Si, Ge; x rational 1/3 (1–4), 2/5 (5), 3/7 (6, 7), ..., $(1 + n)/(3 + 2n)$, ..., 1/2 (8, 9), or irrational 0.360 (10), 0.414 (11), and 0.354 (12)) all derive from a close stacking of $[MTe_2]$ trigonal prismatic slabs. Within the slab, the M metal atoms are either isolated or paired in prisms or biprisms, and the A nonmetal element adopts a Te square environment in the center of otherwise empty biprisms. Each slab is built from zigzagging ribbons with the ... $(M_2)(A)(M_2)(A)$ ... (ribbons **a** and **b**) or ... $(M)(M)$ ... (ribbon **c**) cationic sequences (see Fig. 1). The ... **abcabc** ... ribbon succession leads to the $MA_{1/3}Te_2$ phases (Fig. 1a) and the ... **abab** ... alternation to the $MA_{1/2}Te_2$ phases (Fig. 1f). Several intermediate arrangements give rise to commensurate phases (x rational) such as $MA_{2/5}Te_2$ (Fig. 1c) and $MA_{3/7}Te_2$ (Fig. 1e) or to incommensurately modulated compounds (x irrational) such as MA_xTe_2 ($1/3 < x < 2/5$, Fig. 1b) and MA_xTe_2 ($2/5 < x < 3/7$, Fig. 1d). One clearly sees that the periodicity of the **c** ribbon insertion controls the overall modulation of the structures. The use of superspace group theory helped rationalize the structure determinations (13).

[1] To whom correspondence should be addressed.

The original aim of the MA_xTe_2 phase study was the understanding of the anionic versus cationic electronic band level competition. Indeed, the oxidation states deduced from simple structural and electronic structure considerations (4, 14, 15) do not allow simple charge balances in all cases, except $MA_{1/2}Te_2$ (vide infra). For instance, considering the $MA_{1/3}Te_2$ formulation, the Nb^{3+} and Si^{2+} cation assumption indicates an average oxidation state of −11/12 for each tellurium ion, that is, a charge transfer of 1/6 electron per Te anion. Short bonding Te ··· Te contacts connected to the Te *sp* to *M d* band transfer should occur. Such short Te ··· Te contacts exist in the $MA_{1/3}Te_2$ structures across the van der Waals gap and have been calculated as slightly bonding because of a partial increase in energy of the associated p bands above the Fermi level. Increasing the A content from x = 1/3 to 2/5 and 3/7 reduces the electron deficit count on tellurium from 1/6 to 1/10 and 1/14, respectively. At the $x = 1/2$ limit composition, the charge balance is reached with $M^{3+}A^{2+}_{1/2}Te^{2-}_2$. Therefore one expects the $p \rightarrow d$ charge transfer to smoothly vanish and the associated short interslab Te ··· Te contacts to lengthen toward regular van der Waals distances when x increases from 1/3 to 1/2. The former expectation was correct but the latter proved to be incorrect since the short Te ··· Te contact lengths progressively decrease (9). To elucidate this apparent contradiction, a thorough analysis of the interslab interaction was undertaken. In this contribution, we first report powder pattern characteristics of the MA_xTe_2 compounds that helped us to identify phases and then investigate the genuine origin of the short Te ··· Te interslab contacts in these phases.

POWDER PATTERNS

Since the nonmetal content, x, is limited to the [1/3, 1/2] interval, the stoichiometry difference between two successive MA_xTe_2 phases can be very small (e.g., $MA_{3/7}Te_2$ and $MA_{0.414}Te_2$ or $MA_{1/3}Te_2$ and $MA_{0.360}Te_2$). Accordingly, the synthesis of pure bulk materials is difficult and mixed phase preparations are common. In addition, if the phase characterization is straightforward for single crystals

0022-4596/95 $12.00

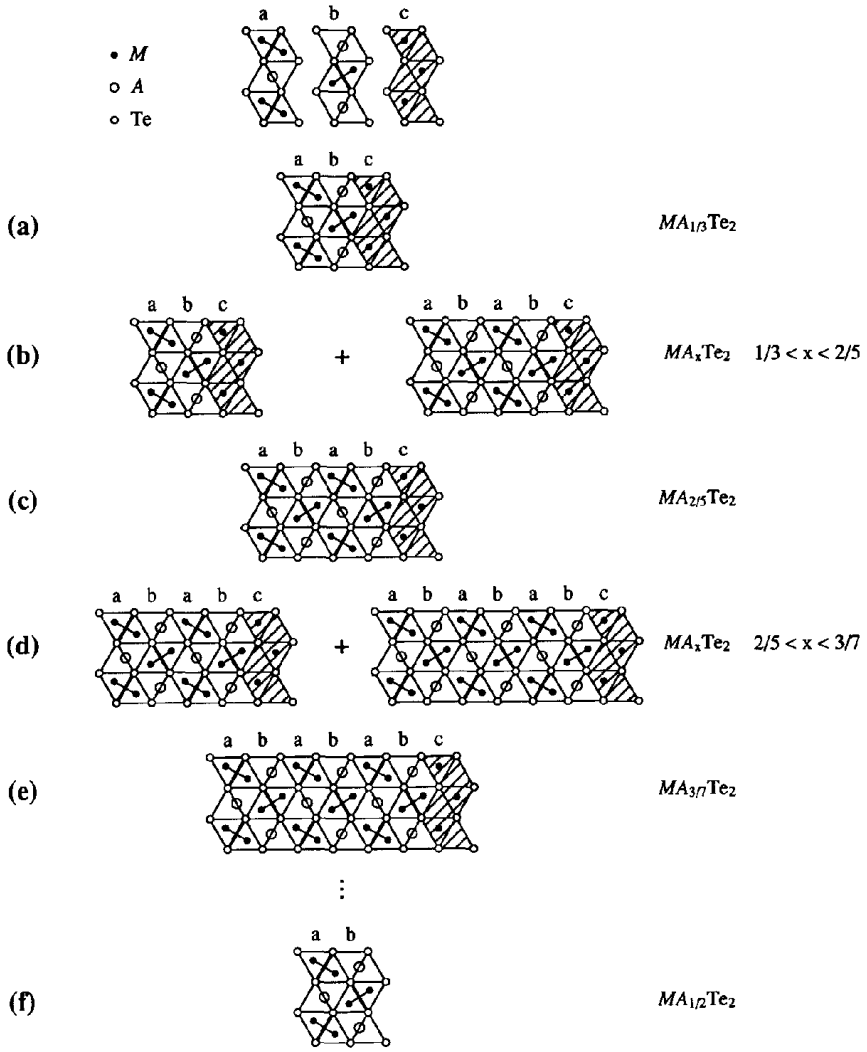

FIG. 1. The three ribbons **a**, **b**, and **c** used to construct the MA_xTe_2 structural slab. The evolution ($a \rightarrow f$) of the slab building as a function of x is shown.

by accurate measurements of the modulation wavevector, it is less obvious from powders because of the similarity of the diffraction patterns and the weakness of the satellite reflections.

Clues to proper phase identifications were given by a close observation of the cell parameters obtained in the course of the structure determinations (see Table 1). Indeed, a significant, linear expansion of the c and b parameters is observed within each homologous series. The c variation can be evaluated on the basis of the difference in width of the **a** (or **b**) and **c** ribbons. For instance, within the $NbGe_xTe_2$ series, an **a** (**b**) ribbon average width ($w_a^{Nb/Ge}$) of 3.9613 Å is calculated from the c cell parameter of $NbGe_{1/2}Te_2$ which does not have **c** ribbons. Assuming the same width in all $NbGe_xTe_2$ phases, a width of $w_c^{Nb/Ge}$ = 3.6013 Å is deduced for a **c** ribbon in $NbGe_{1/3}Te_2$. This allows one to predict the average c parameter for any stoichiometry x:

$$c_{\text{average}} = 2w_a^{Nb/Ge}x + w_c^{Nb/Ge}(1 - 2x).$$

With this equation, c parameters of 3.8893 and 3.9099 Å are predicted for x = 2/5 and 3/7, respectively, in very good agreement with the observed values of 3.8936 and 3.9072 Å, respectively. Similar values can be obtained for the homologous $TaSi_xTe_2$ series, i.e.,$w_a^{Ta/Si}$ = 3.9315 Å and $w_c^{Ta/Si}$ = 3.5508 Å, and the $NbSi_xTe_2$ series, i.e., $w_a^{Nb/Si}$ = 3.9440 Å and $w_c^{Nb/Si}$ = 3.6191 Å. Unfortunately, since an accurate determination of the c lattice parameter of the average cell from powder patterns requires a full analysis of the diagrams, this procedure is ruled out when dealing with a phase mixture.

TABLE 1
MA_xTe_2 Cell Parameters Obtained from Single Crystal Reflection Centering

Formula	a (Å)	b (Å)[a]	c (Å)	V (Å^3)[b]
$NbSi_{1/3}Te_2$ (3)	6.353(2)	13.938(5)	3.8357(13)	339.6(2)
$NbSi_{1/2}Te_2$ (8)	6.336(1)	14.079(2)	3.9440(8)	351.8(1)
$NbGe_{1/3}Te_2$ (2)	6.435(2)	13.915(4)	3.8413(7)	344.0(3)
$NbGe_{2/5}Te_2$ (5)	6.4437(9)	13.984(2)	3.8936(4)	350.85(7)
$NbGe_{3/7}Te_2$ (6)	6.435(1)	14.006(2)	3.9072(4)	352.15(8)
$NbGe_{1/2}Te_2$ (9)	6.448(2)	14.082(2)	3.9613(6)	359.7(1)
$TaSi_{1/3}Te_2$ (4)	6.329(1)	14.010(3)	3.8046(10)	337.6(1)
$TaSi_{0.360}Te_2$ (10)	6.329(3)	14.031(3)	3.8258(7)	339.7(2)
$TaSi_{0.414}Te_2$[c]	6.332(4)	14.080(1)	3.8689(4)	344.9(3)
$TaSi_{3/7}Te_2$ (7)	6.339(1)	14.115(3)	3.8771(6)	346.9(1)
$TaGe_{0.354}Te_2$ (12)	6.440(1)	14.023(2)	3.8461(5)	347.3(2)

[a] For the sake of comparison, all parameters have been established in the same orthogonal reference basis (although some real cells are monoclinic).
[b] Volume of the average cell.
[c] New set of cell parameters, different from parameters in Ref. (11).

The b stacking parameter (in an orthogonal basis) varies to a lesser extent but can be easily determined from the $0k0$ reflection set. Indeed, the $0k0$ lines can conveniently be singled out in a flat plate X-ray diffraction geometry because of the 2D nature of the material (increasing the preferred orientation can be achieved by pressing the powder onto the sample holder cavity). This is shown in Fig. 2 where the $0k0$ line groups (040, 060, and 080) of a $NbGe_xTe_2$ phase mixture obviously stand out. An expansion of the 080 line group is presented in Fig. 3 along with the least-squares refined profiles. Although very close in stoichiometry, the four $NbGe_xTe_2$ phases of the mixture (x = 1/3, 2/5, 3/7, and 1/2) give rise to well-resolved 080 peaks. In addition, the line positions (in Å) perfectly follow the x stoichiometry parameter as shown in Fig. 4. This dependence of b upon the stoichiometry proved very helpful in identifying pure phases. Indeed, phases with a 1% difference in x give a 0.015° (2θ) shift around 50°, large enough to be noticed on a high-resolution powder pattern. Such an analysis was always performed prior to any pattern indexing and cell parameter refinement.

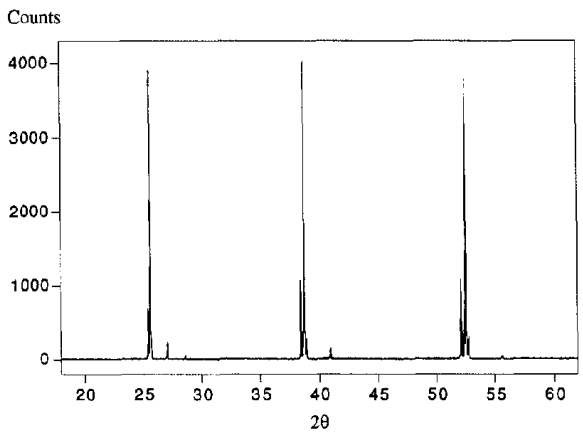

FIG. 2. Powder pattern of a $NbGe_xTe_2$ phase mixture [data collection on a Siemens D5000 diffractometer (CuK–L_3)]. Since the sample was purposely pressed onto the cavity to emphasize the preferred orientation, the powder pattern almost exclusively shows the $0k0$ lines.

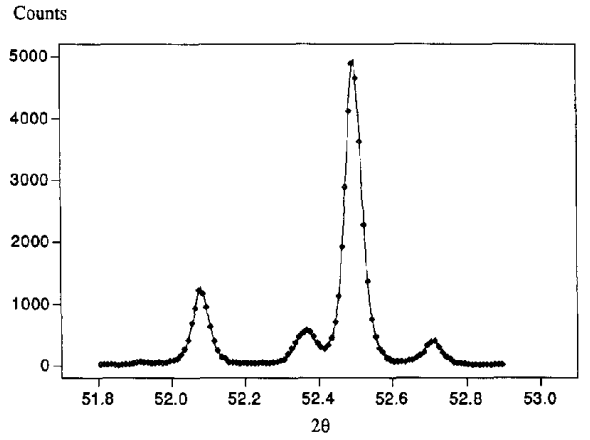

FIG. 3. Experimental and calculated 080 lines of four $NbGe_xTe_2$ phases [x = 1/3, 2/5, 3/7, and 1/2; data collection on a Siemens D5000 diffractometer (CuK–L_3); pseudo-Voigt lineshape].

SHORT INTERSLAB Te ··· Te CONTACTS AND CHARGE TRANSFER

As mentioned in the Introduction, a striking feature of the MA_xTe_2 structures is the evolution of the short in-

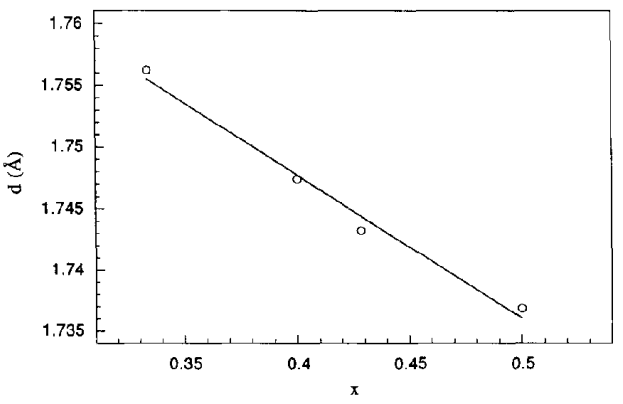

FIG. 4. The 080 interplanar distance (d) versus stoichiometry (x) in the four $NbGe_xTe_2$ phase mixture (x = 1/3, 2/5, 3/7, and 1/2).

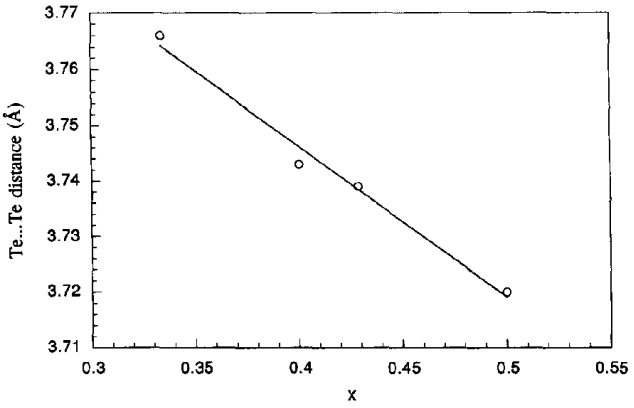

FIG. 5. Evolution of the shortest interslab Te ··· Te distance as a function of x in the homogenous $NbGe_xTe_2$ series.

terslab Te ··· Te distance as a function of x (reproduced in Fig. 5 for the $NbGe_{2/5}Te_2$ homologous series). For $x < 1/2$ one does expect some interslab Te–Te contacts to be shorter than the regular van der Waals distance of 4.1 Å. Indeed, it has been shown (4, 14) that, for $x < 1/2$, the partial $p \rightarrow d$ electron transfer required to balance the charges is achieved by a shortening of the Te ··· Te interslab contacts, inducing a depletion of the antibonding top of the tellurium p band. However, if it is maximum for $x = 1/3$, the electron transfer is expected to vanish for $x = 1/2$, and accordingly the Te ··· Te interslab contacts are expected to lengthen. Indeed, the electron transfer actually stops for $x = 1/2$ since, for that limiting stoichiometry, the tellurium p band is filled. In addition, for this same limiting stoichiometry, negative overlap populations are calculated for the short interslab Te ··· Te contacts (9). To understand the origin of the actual shrinking of the shortest interslab Te ··· Te distances, a thorough analysis of the slab stacking is necessary.

A projection, perpendicular to the layer plane, of two sandwich slabs of $NbGe_{2/5}Te_2$ is presented in Fig. 6. To improve the legibility of the figure, the upper slab (top of Fig. 6), the interslab Te–Te interaction (middle of Fig. 6), and the lower $NbGe_{2/5}Te_2$ slab (bottom of Fig. 6) are singled out. The shortest Te–Te contacts within and parallel to the slab (3.32 Å, type I) and across the van der Waals gap (3.74 and 3.81 Å, type II) are highlighted as black solid lines. One easily recognizes the Te(I–II–I) and Te(I–I) contact patterns described in (11). There is a complete correlation between the short interslab type II Te ··· Te contacts and the modulation of the tellurium positions, because it follows the cation filling of the prismatic tellurium sites within each slab, that is, either lone Nb atoms, Nb_2 pairs, or Ge atoms. In MA_xTe_2 phases with high x value, in particular in $NbGe_{1/2}Te_2$ in which no transfer occurs and no interslab Te ··· Te bonds are present (as demonstrated by the charge balance and the negative electronic overlap population between telluriums (9)), such short type II Te ··· Te contacts should be lengthened.

One way to do so would be for the structure to increase the van der Waals gap width. However, to minimize the total energy an average interslab Te ··· Te distance must be maintained as close as possible to the regular van der Waals distance of 4.1 Å. Therefore, the van der Waals gap widening, and correlatively the stacking parameter, should be strongly correlated to the density of type II contacts, i.e., important for a large density and minimum for a small density. Since such a density has been shown (11) to steadily decrease with x (although remaining quite low as compared to the total number of Te ··· Te interslab contacts, that is, 1/9 and 1/12 for $x = 1/3$ and 1/2, respectively), the stacking parameter is expected to diminish with x. This is not what is experimentally observed, as indicated by the b values gathered in Table I.

Another possibility would be a displacement of only the involved atoms away from each other, that is, toward the cationic trigonal prismatic slab. Such a displacement implies that the Te atoms "enter" the cationic slab, which is only possible if there are no Nb–Te or Nb–Ge bondings. All Te atoms have similar contacts except those participating in the **c** ribbon (16). Indeed, as can be seen in Fig. 6, the latter atoms (shaded) coordinate an empty trigonal prism and, therefore, can be easily displaced toward that empty site.

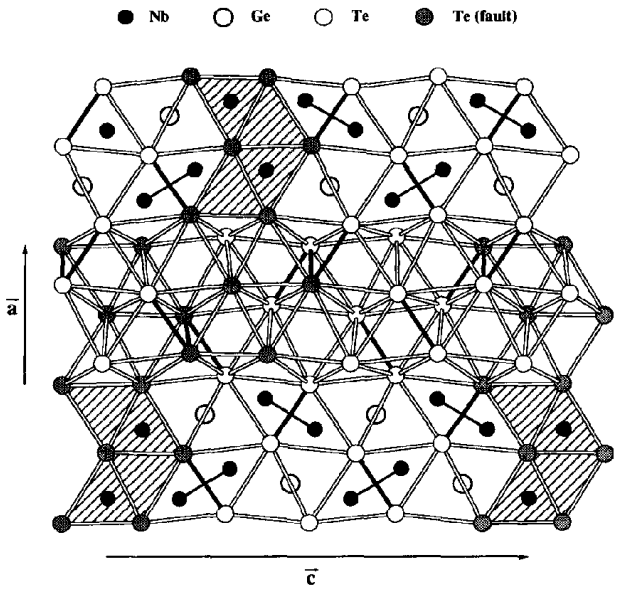

FIG. 6. Projection, perpendicular to the layer plane, of two $NbGe_{2/5}Te_2$ slabs. The upper slab, the lower slab, and the interslab Te ··· Te interaction are shown in the top, the bottom, and the middle of the figure, respectively. The shortest intra- and interslab Te ··· Te contacts are indicated by thick solid lines, showing the Te(I–II–I) and Te(I–I) patterns (11). The **c** ribbons (faults) and the Te atoms neighboring them are shaded.

TABLE 2
Te y Coordinates versus Coordination in $NbGe_{2/5}Te_2$

Center of slab: 0.25; center of gap: 0.0

Te not involved in type II Te ··· Te contacts:
0.11686, 0.11428, 0.11374, 0.11353, 0.11698, 0.11531, 0.11400 (average 0.11496)

Te involved in type II Te ··· Te′ contacts:

(i)	both Te and Te′ participating in **c** ribbons	0.12093 (Te ··· Te′ of 3.813 Å)
(ii)	Te participating in **c** ribbons but not Te′	0.11927 (Te ··· Te′ of 3.743 Å)
(iii)	Te′ participating in **c** ribbons but not Te	0.11532 (Te ··· Te′ of 3.743 Å)
(iv)	neither Te nor Te′ participating in **c** ribbons (not occurring in $NbGe_{2/5}Te_2$ but a simulation gives a Te ··· Te′ distance of 3.68 Å)	

In fact, both possibilities (gap width increase and site displacement) are at work in most MA_xTe_2 phases, as illustrated by the $NbGe_{2/5}Te_2$ structure. From Table 2 and Fig. 7, it can be seen that all Te atoms not involved in type II Te ··· Te contacts have roughly the same elevation (0.11496 on average). For those involved in type II Te ··· Te′ short contacts, four different situations can occur. First, both Te and Te′ are at the border of a **c** ribbon (Fig. 7a). Therefore, they can both move slightly inside their slab (as indicated by the increase in y(Te) from the average value of 0.11496 to 0.12093). Next, only one tellurium atom of the contact, Te or Te′, is at the edge of a **c** ribbon (Figs. 7b and 7c). Hence, that particular atom can be displaced (from 0.11496 to 0.11927; see Table 2), with the other atom remaining around the average elevation (0.11532; see Table 2). As a consequence, the type II contact is shorter than that of the former situation (3.74 instead of 3.81 Å). Finally, neither Te nor Te′ are at the border of a **c** ribbon (Fig. 7d). This situation is not encountered in $NbGe_{2/5}Te_2$ (it is in $NbGe_{1/2}Te_2$) but can easily be simulated by choosing appropriate coordinates. Since none of the Te atoms can be displaced, this would lead to a much shorter distance of 3.68 Å. Such a short distance can be considered for other compositions as well; it is calculated to be 3.67 for $x = 1/3$ and observed at 3.72 Å for $x = 1/2$. This clearly indicates that a parameter expansion also contributes to the elongation of otherwise quite short distances.

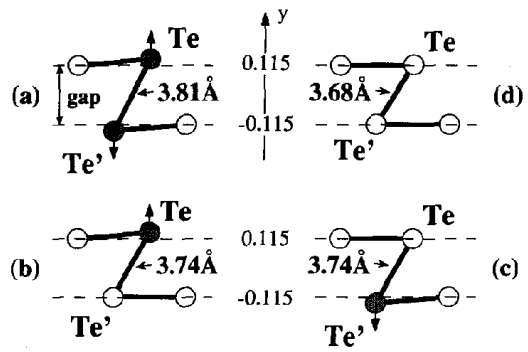

FIG. 7. Te displacement and Te ··· Te interslab distance as a function of coordination in $NbGe_{2/5}Te_2$. Te atoms neighboring the **c** ribbons (shaded) can be displaced toward the cationic slab, therefore increasing the Te ··· Te interslab distance (see Table II for proper y coordinates).

For $x = 1/3$ a charge transfer is at play, depleting the antibonding top of the p_z band of the tellurium atoms of type II short contacts. A distance shorter than the usual van der Waals contact (4.1 Å) is then expected (14). In addition, each "type II" Te atom can move toward a **c** ribbon. Therefore, for $NbGe_{1/3}Te_2$ one expects no or weak parameter expansion along the stacking direction. In contrast, for $x = 1/2$ no charge transfer should occur since charge balance is achieved and the Te p_z band is filled (9). Hence, one does not expect short Te ··· Te contacts through the van der Waals gap. However, since each "type II" Te atom is confined within the average Te plane because there are no **c** ribbons in that structure, the only way to lengthen the short antibonding interslab Te ··· Te contacts and maximize the van der Waals energy interaction is to increase the van der Waals gap width. Since the density of type II Te ··· Te contacts is small, the expansion is not sufficient to bring the Te–Te distance back to the usual values and the distance remains short, in fact the shortest of the whole series. This fully explains the stacking parameter expansion with x seen in Table 1 and the apparently contradictory shrinking of the shortest interslab Te ··· Te contacts as a function of x (Fig. 5). It also explains the necessity of a slight surface reconstruction in the interpretation of the scanning tunneling microscopy images.

In previous studies (4, 8, 14), it has been stated that, in the MA_xTe_2 phases, the charge transfer is realized through the creation of short interlayer Te ··· Te contacts. Obviously, this statement should be reconsidered. Indeed, short interlayer Te ··· Te contacts do exist in all the MA_xTe_2 phases because of steric effects, with or without charge

transfers. However, it is true to say that the short interslab contacts raise the associated p_z tellurium orbital levels well above the other tellurium levels and that, if a charge transfer takes place, it will occur from a depletion of those levels.

REFERENCES

1. L. Monconduit, M. Evain, F. Boucher, R. Brec, and J. Rouxel, *Z. Anorg. Allg. Chem.* **616,** 177 (1992).
2. J. Li and P. J. Caroll, *Mater. Res. Bull.* **27,** 1073 (1992).
3. J. Li, M. E. Badding, and F. J. DiSalvo, *J. Alloys Compounds* **184,** 257 (1992).
4. M. Evain, L. Monconduit, A. van der Lee, R. Brec, J. Rouxel, and E. Canadell, *New J. Chem.* **18,** 215 (1994).
5. A. van der Lee, M. Evain, M. Mansuetto, L. Monconduit, R. Brec, and J. Rouxel, *J. Solid State Chem.* **111,** 75 (1994).
6. A. van der Lee, M. Evain, L. Monconduit, R. Brec, and S. van Smaalen, *J. Phys. Condens. Matter* **6,** 933 (1994).
7. M. Evain, L. Monconduit, and A. van der Lee, in preparation.
8. L. Monconduit, M. Evain, R. Brec, J. Rouxel, and E. Canadell, *C.R. Acad. Sci. Paris* **314,** 25 (1993).
9. J. Gareh, F. Boucher, and M. Evain, in preparation.
10. A. van der Lee, M. Evain, L. Monconduit, R. Brec, J. Rouxel, and V. Petříček, *Acta Crystallogr. Sect. B* **50,** 119 (1994).
11. M. Evain, A. van der Lee, L. Monconduit, and V. Petříček, *Chem. Mater.* **6,** 1776 (1994).
12. F. Boucher, M. Evain, L. Monconduit, and V. Petříček, in preparation.
13. A. van der Lee and M. Evain, *in* "Aperiodic '94, Conference Proceedings," (G. Chapuis and W. Paciorek, Eds.), p. 440. World Scientific Publishing, 1995.
14. E. Canadell, L. Monconduit, M. Evain, R. Brec, J. Rouxel, and M.-H. Whangbo, *Inorg. Chem.* **32,** 10 (1993).
15. J. Rouxel and M. Evain, *Eur. J. Solid State Inorg. Chem.* **31,** 683 (1994).
16. H. Bengel, H.-J. Cantow, S. N. Magonov, L. Monconduit, M. Evain, W. Liang, and M.-H. Whangbo, *Adv. Mater.* **6,** 649 (1994).
17. W. Liang, M.-H. Whangbo, M. Evain, L. Monconduit, R. Brec, H. Bengel, H.-J. Cantow, and S. N. Magonov, *Chem. Mater.* **6,** 678 (1994).